Journal of the European Ceramic Society **18** (1998) 501–508

PII: S0955-2219(97)00164-7
0955-2219/98/$19.00 + 0.00

Pinning Effect of SiC Particles on Mechanical Properties of Al_2O_3–SiC Ceramic Matrix Composites

Zhen-Yan Deng,* Jian-Lin Shi, Yu-Feng Zhang, Dan-Yu Jiang and Jing-Kun Guo

The State Key Laboratory of High Performance Ceramics and Superfine Microstructure,
Shanghai Institute of Ceramics, Chinese Academy of Sciences, Shanghai 200050, People's Republic of China

(Received 14 February 1997; accepted 11 August 1997)

Abstract

The fracture mechanical properties of SiC particle reinforced Al_2O_3 matrix composites were investigated at room temperature and $T = 1200°C$. The results showed that the fracture strength and toughness of composites are enhanced, compared with those of monolithic Al_2O_3, especially at elevated temperature, and the strength and toughness of composites increase with the increase in the content of SiC particles. It was found that the improvement in fracture mechanical properties of composites is due to the fracture mode transformation from intergranular in monolithic Al_2O_3 to transgranular in the composites, and the fracture mode change might result mainly from the pinning effect of SiC particles on the Al_2O_3 boundaries. The study on flexure creep behavior of monolithic Al_2O_3 and the composites with 20 vol% SiC particles at $T = 1260°C$ indicated that the composites also exhibited some improvement in their creep resistance, compared to the creep behavior of monolithic Al_2O_3, due to the pinning effect of SiC particles at Al_2O_3 grain boundaries on grain boundary sliding during creeping. © *1998 Elsevier Science Limited. All rights reserved*

1 Introduction

Since the pioneer work of Niihara,[1] nanometer-sized SiC particle reinforced Al_2O_3 matrix composites have received considerable attention in the past few years.[2–11] The investigation of Niihara[1] reported that as little as 5 vol% of 0·3 μm SiC particles could increase the strength of hot-pressed alumina from 350 MPa to over 1 GPa and the fracture toughness from 3·25 to 4·70 MPa$\times$m$^{1/2}$, and further annealing enhances the strength of this nanocomposite to 1·5 GPa. Niihara[1] proposed a variety of mechanisms to explain this behavior, including crack deflection, sub-grain-boundary formation and microcracking. Subsequent work of Harmer's group[2,3] confirmed the strengthening of alumina by SiC nanoparticles, but the toughness increase was modest and not sufficient to account for the vast improvement in strength. They suggested that the apparent strengthening arises from machining-induced compressive surface stress, and the further strength increase of nanocomposites after heat treatment results from the healing of machining flaws during annealing. The surface stress, stress relaxation and crack healing of nanocomposites were verified by their recent work.[7,8,10] On the other hand, the investigation of Anya and Roberts[11] on the Al_2O_3–SiC nanocomposites showed that the fracture toughness of nanocomposites increases apparently, in comparison to that of monolithic Al_2O_3. The theoretical analysis by Levin *et al.*[6] indicated that the strengthening and toughening in the Al_2O_3–SiC nanocomposites could be attributed to the change in the fracture mode from intergranular in monolithic Al_2O_3 to transgranular in nanocomposites, and it was suggested that this change in fracture mode is a result of matrix weakening and grain boundary strengthening, due to the thermal residual stress produced by the thermo-elastic mismatch between Al_2O_3 and SiC.

In our previous paper,[12] we have studied the microstructure and creep behavior of 10 vol% SiC particle reinforced Al_2O_3 matrix composites for the SiC particles with different SiO_2 impurities. In this study, we report the results of the fracture mechanical behavior of the Al_2O_3–SiC composites at room and elevated temperature and the creep

*To whom correspondence should be addressed.

behavior of the composites with 20 vol% SiC particles.

2 Experimental

As in our previous paper,[12] two kinds of SiC particles were used in this study: one with the average size of 0·6 μm and the other with the average size of 2·7 μm, which are represented by S and L hereafter. The main impurity in SiC particles is SiO_2, 1·7 vol% and 3·4 vol% SiO_2 were in S and L SiC particles, respectively, and the impurity content per unit area on the surface of the latter is about one order of magnitude higher than that on the former.[12] The monolithic Al_2O_3 and composites were fabricated by hot-pressing at 20 MPa in flowing Ar atmosphere at 1700°C for 30 min.

The dense monolithic Al_2O_3 and composite tiles were ground and sectioned into $3\times4\times30\,mm^3$, $2{\cdot}5\times5\times30\,mm^3$ and $2\times4\times40\,mm^3$ test bars with the edges chamfered for strength, toughness and flexure creep tests, respectively. Density measurement of the specimens were made using the Archimedes technique in distilled water. The densities of monolithic Al_2O_3 and four kinds of composites were all over 99·5% of theoretical densities. The fracture strength was determined by the three-point bending method with a span of 20 mm and at a loading rate of 0·5 mm min^{-1}. The fracture toughness was measured using the single edge-notched beam test, with the notch depth of 2·5 mm and notch width of 0·2 mm. The high temperature strength and toughness were measured at T = 1200°C in air atmosphere. The data of strength and toughness are the average of at least three specimens. The flexure creep tests were conducted in air atmosphere at 1260°C, and only monolithic Al_2O_3 and the composites with 20 vol% SiC particles were used for the creep tests. The creep experimental apparatus have been described in our previous paper,[12] and the specimens were loaded in a four-point flexure fixture made of high-purity SiC with inner and outer span lengths of 10 and 30 mm, respectively. Specimens were held at testing temperature for at least 30 min prior to applying the load. The number of the creep specimens for monolithic Al_2O_3 or each type of composites is at least three in order to study the variations in creep rate with stress.

The features of fracture surface and the microstructures of as-fabricated and crept specimens were analyzed by scanning electron microscopy (SEM) and transmission electron microscopy (TEM). The average Al_2O_3 matrix grain size for monolithic Al_2O_3 and composites was measured using the method similar to that of O'Donnell *et al.*[13] We first measured the grain area from several representative SEM or TEM micrographs consisting of at least 250 grains for monolithic Al_2O_3 or each kind of composites, and calculated the grain diameter using the measured grain area by equating the grain to a spherical particle, and then averaged the grain size. The average grain size was multiplied by 1·5 to account for stereological effect resulting from the two-dimensional measurements.

3 Results and discussion

3.1 Al_2O_3 grain morphology of composites

The results of our previous paper[12] showed that the grains of monolithic Al_2O_3 are equiaxed, and with an uniform grain-size distribution. The composite with 10 vol% SiC(S) particles (ASS1) is also mainly equiaxed, but the elongated matrix grains can be seen occasionally, and most of its SiC particles are on the Al_2O_3 grain boundaries or triple-grain junctions. However, the grain morphology of the composite with 10 vol% SiC(L) particles (ASL1) is irregular and most of its Al_2O_3 matrix grains are elongated, and the SiC particles in ASL1 are mainly entrapped into the Al_2O_3 grains. The recent investigation[14] indicated that the irregular grain morphology and the entrapment of SiC particles into Al_2O_3 grains in ASL1 is due to the higher content of SiO_2 impurity existed on 2·7 μm SiC particle surfaces which impedes the Al_2O_3 grain boundary movement around the SiC particles during hot-pressing.

The grain morphology of the composites with 20 vol% SiC particles is different from that of ASL1, and similar to that of ASS1, as shown in Fig. 1. Figure 1 shows that the composite with 20 vol% SiC(S) particles (ASS2) and with 20 vol% SiC(L) particles (ASL2) both have an uniform grain-size distribution and equiaxed grain morphology, and their SiC particles are not entrapped into the Al_2O_3 matrix grains. Although the higher SiO_2 impurity content on 2·7 μm SiC particle surfaces caused the Al_2O_3 grain morphology of ASL1 to be irregular and elongated, the grain morphology of ASL2 is equiaxed. This is due to the higher volume content of SiC particles in ASL2, which makes the matrix Al_2O_3 grain size of ASL2 much smaller than that of ASL1, as listed in Table 1, because the inhibition effect of SiC particles on Al_2O_3 grain growth increases with the increase in the volume content of SiC particles in the composites.[4] In fact, the SiC grain size in ASL2 is comparable to that of Al_2O_3 matrix grains, and the Al_2O_3 matrix grains in ASL2 are not large enough to enclose the 2·7 μm SiC particles. In addition, the

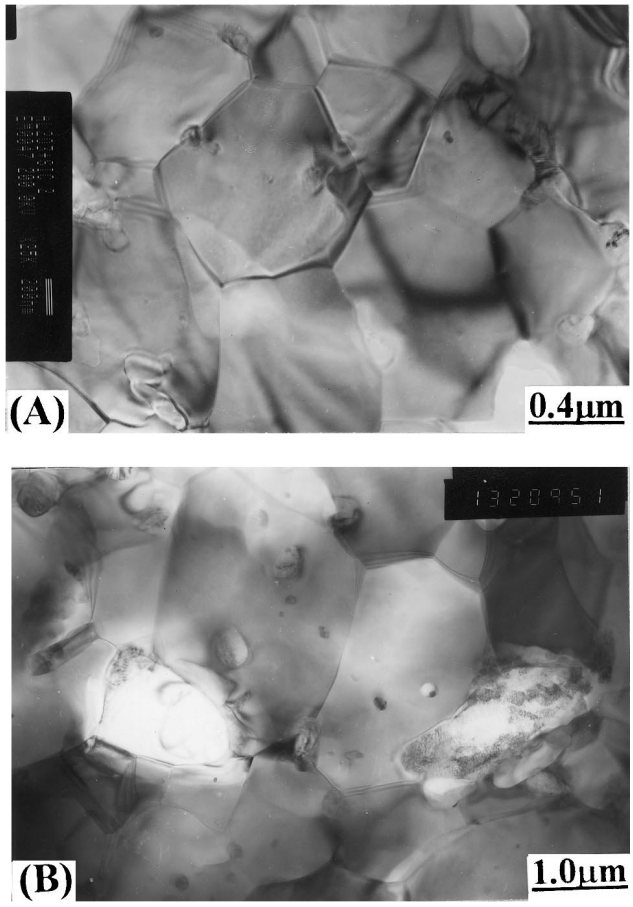

Fig. 1. TEM micrographs of (A) ASS2 and (B) ASL2, showing the equiaxed grain morphology of the composites with 20 vol% SiC particles.

Al_2O_3 grain size of the composites with 2·7 μm SiC particles is smaller than that with 0·6 μm SiC particles for the same volume content of SiC particles, which may result from the fact that the coarser inclusions impede grain growth less by virtue of the smaller number of grains occupying the grain boundary for an equivalent volume percentage of the second phase.[4]

3.2 Mechanical properties and fracture morphology

Table 1 also lists the fracture strength and toughness of monolithic Al_2O_3 and the composites with different size and content of SiC particles at room temperature. From Table 1, we can see that the fracture strength and toughness of the composites with 10 vol% SiC particles are slightly higher than those of monolithic Al_2O_3, and the fracture strength and toughness of the composites with 20 vol% SiC particles exceeds those of monolithic Al_2O_3 by about 20%, independent of the size of SiC particles added. Table 2 shows the fracture strength and toughness of monolithic Al_2O_3 and composites at T = 1200°C. In general, the fracture strength and toughness at T = 1200°C decrease, compared with those at room temperature, but the degradation in strength and toughness at elevated temperature for the composites is lower than those for monolithic Al_2O_3. Table 2 indicates that the high temperature strength of composites exceeds that of monolithic Al_2O_3 by about 30%, and the high temperature fracture toughness of the composites exceeds that of monolithic Al_2O_3 by about 50%, especially for ASL1 with the high temperature fracture toughness exceeding that of monolithic Al_2O_3 by over 90%.

Figures 2 and 3 show the fracture features of monolithic Al_2O_3 and the composites at room and elevated temperature, respectively. In Figs 2(A) and 3(A), it is apparent that the fracture mode for monolithic Al_2O_3 at room and elevated temperature is intergranular, the transgranular fracture is seldom found in their fracture surfaces. In Figs 2(B)–(E) and 3(B)–(E), it can be also seen that the fracture mode for the composites is mainly transgranular at room and elevated temperature, though the fracture surfaces of the composites at T = 1200°C are not very clear due to the oxidation reaction of the surface SiC particles, and higher volume content of SiC particles in the composite leads to higher extent of the transgranular fracture on its fracture surface.

3.3 Toughening mechanisms

The results of Hansson *et al.*[15] showed that the fracture mode change in Al_2O_3 from intergranular to transgranular increases the fracture toughness to be about $\Delta K_T = 0{\cdot}58K_0$, where K_0 is the fracture toughness of monolithic Al_2O_3, and the change in fracture mode alone can account adequately for the increase in fracture toughness of the composites. It can be concluded that the fracture mode

Table 1. The average matrix grain size of monolithic Al_2O_3 and composites, and their fracture strength and toughness at room temperature

Materials	*Grain size, d (μm)*	$d_{alumina}/d_{composite}$	σ_f *(MPa)*	$K_{IC}(MPa\times m^{1/2})$ *(measured)*	$K_{IC}(MPa\times m^{1/2})$ *(predicted)*
Al_2O_3	7·61	—	457	5·17	—
Al_2O_3/10 vol%SiC(S)	4·99	1·53	477 (104%)	5·47 (106%)	6·36 (123%)
Al_2O_3/20 vol%SiC(S)	1·83	4·16	574 (126%)	6·31 (122%)	7·40 (143%)
Al_2O_3/10 vol%SiC(L)	6·68	1·14	458 (100%)	5·44 (105%)	6·02 (116%)
Al_2O_3/20 vol%SiC(L)	2·74	2·78	619 (135%)	6·16 (119%)	6·87 (133%)

The data in the parentheses are the ratios of the fracture strength or toughness of composites to that of monolithic Al_2O_3

Table 2. Fracture strength and toughness of monolithic Al_2O_3 and composites T = 1200°C

Materials	σ_f *(MPa)*	K_{IC} *(MPa×m$^{1/2}$) (measured)*	K_{IC} *(MPa×m$^{1/2}$) (predicted)*
Al_2O_3	352	2·46	—
Al_2O_3/10 vol%SiC(S)	454 (129%)	3·67 (149%)	3·17 (129%)
Al_2O_3/20 vol%SiC(S)	459 (130%)	4·25 (173%)	3·74 (152%)
Al_2O_3/10 vol%SiC(L)	451 (128%)	4·69 (191%)	3·17 (129%)
Al_2O_3/20 vol%SiC(L)	501 (142%)	3·76 (153%)	3·74 (152%)

The data in the parentheses are the ratios of the fracture strength or toughness of composites to that of monolithic Al_2O_3.

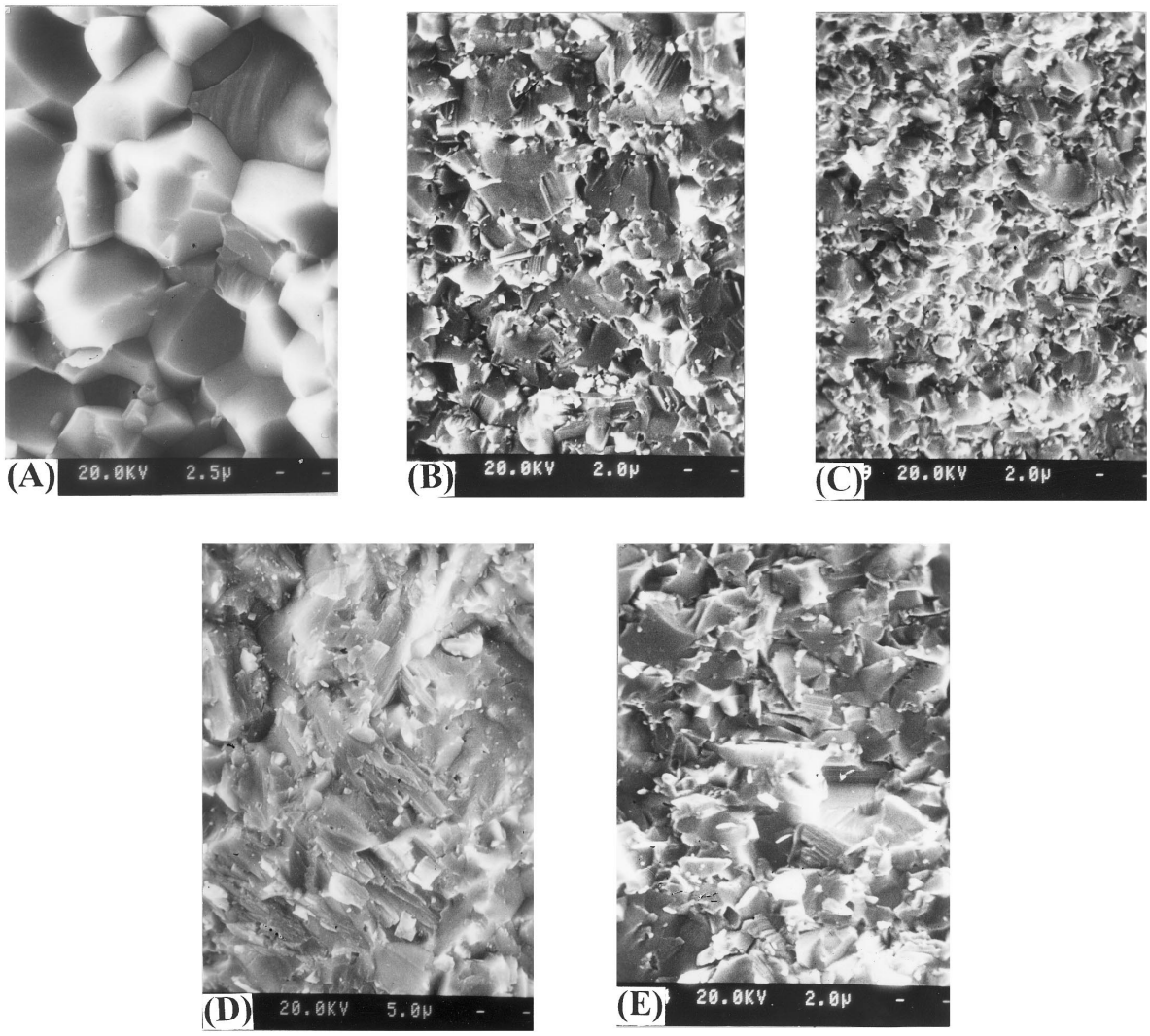

Fig. 2. SEM micrographs of the fracture surfaces at room temperature: (A) monolithic Al_2O_3, (B) ASS1, (C) ASS2, (D) ASL1 and (E) ASL2.

transformation is the dominant factor responsible for the increase in the fracture toughness of the composites at room and elevated temperature. Crack deflection may not be an important factor for the toughening of the composites,[6] because the transgranular fracture might make the crack path more direct in the composites than that in monolithic Al_2O_3.

The results of Levin *et al.*[6] indicated that the fracture mode change for the Al_2O_3–SiC nanocomposites results from the matrix weakening and grain boundary strengthening, because the thermal residual stress in the Al_2O_3 matrix is tensile and the local residual stress normal to the Al_2O_3/SiC interface is compressive, which are favorable for the transgranular fracture in the nanocomposites. However, the investigation of Ohji *et al.*[9] showed that the much stronger Al_2O_3/SiC interface bonding may be the principal mechanism responsible for the transgranular fracture in nanocomposites,[9] due to the strong bonding between Al_2O_3 and SiC also inhibiting the crack to propagate along the Al_2O_3/SiC interface. For the composites in this study, the cause responsible for the fracture mode transformation may be the pinning effects of SiC particles on Al_2O_3 grain boundaries, because part of the SiC

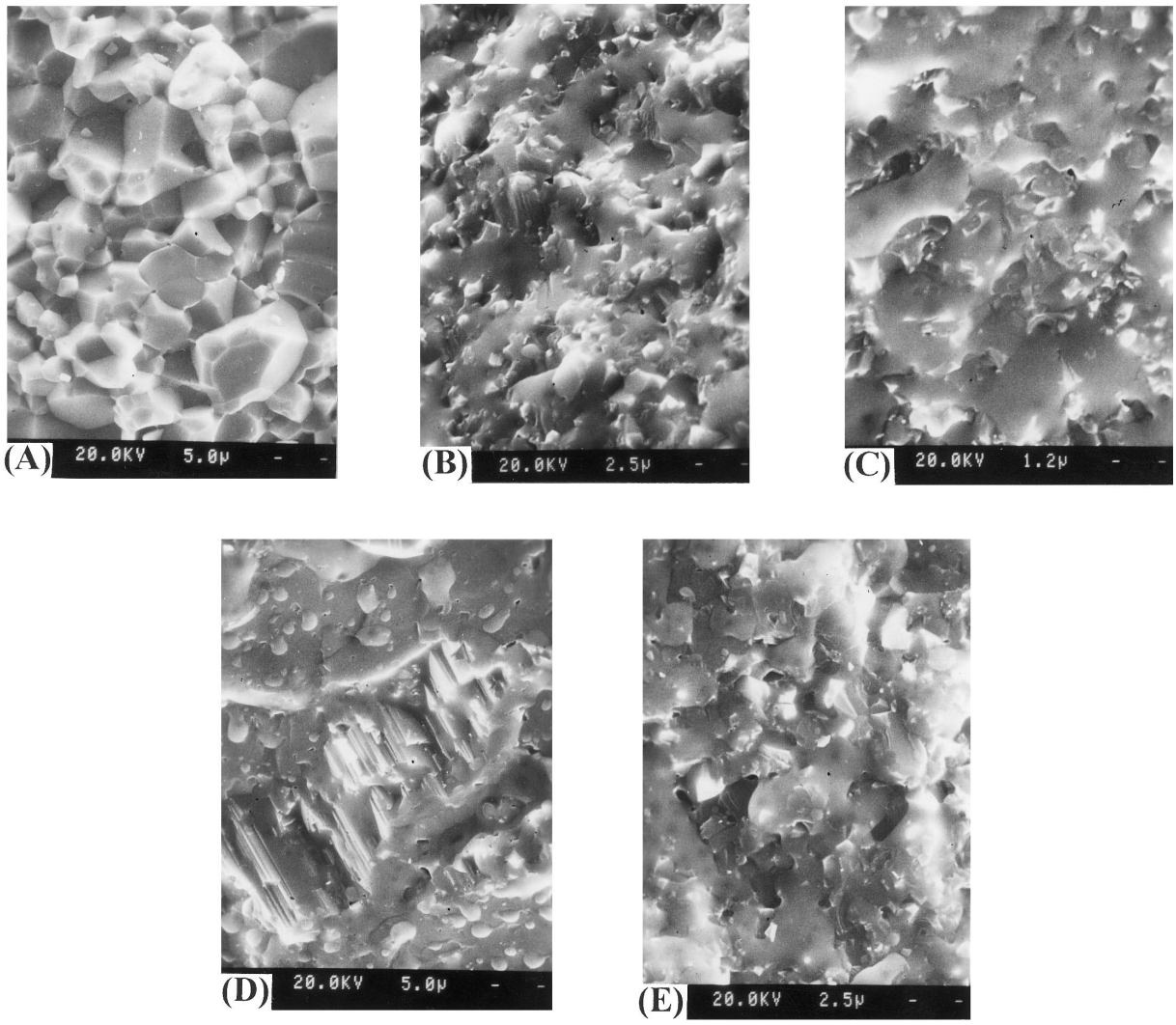

Fig. 3. SEM micrographs of the fracture surfaces at T = 1200°C: (A) monolithic Al_2O_3, (B) ASS1, (C) ASS2, (D) ASL1 and (E) ASL2.

particles are irregular and elongated, as shown in Fig. 4, which interlock the Al_2O_3 grain boundaries and would impede the crack extension along the Al_2O_3 interfaces, similar to the pinning effect of SiC whiskers. In fact, the residual stress in composites almost vanishes at elevated temperature, but the transgranular fracture also existed on their fracture surfaces at elevated temperature, and the interface bonding between Al_2O_3 and SiC in the present composites[14] is not as good as that in the Al_2O_3–SiC nanocomposites;[9] so the residual stress and interface bonding may not be the principal mechanisms responsible for the fracture mode transformation in the present composites.

Considered the fracture mode transformation and the thermal residual stress, the total fracture toughness of composites can be written

$$K_{IC} = K_0 + \Delta K_R + \alpha \Delta K_T \qquad (1)$$

where α is the fraction of transgranular fracture on the fracture surfaces of composites, and

$$\Delta K_R = 2q[2(\lambda - d)/\pi]^{1/2} \qquad (2)$$

is the contribution of thermal stress field to the toughness of composites.[16] In eqn (2), q is the average residual stress in the matrix, $\lambda = 1{\cdot}085 \times d/\left(f_p\right)^{1/2}$ is the distance between reinforcing particles with d the grain size and f_p the fraction of particle volume. The average residual tensile stress in the matrix can be obtained by the formulas developed by Taya *et al.*,[16] the material parameters (thermal expansion coefficient, elastic constant and Poisson's ratio) used in this study are the same as those used by Levin *et al.*,[6] and the temperature difference forming the residual stress adopted in this study is $\Delta T = 1200$°C. As the matrix residual stress in the composites is tensile,[6] which is beneficial to the crack propagation, and the residual stress would decrease the toughness of the composites. At elevated temperature, the residual stress in the composites vanishes and the negative effect of residual stress on the fracture toughness of the composites is zero, which may be

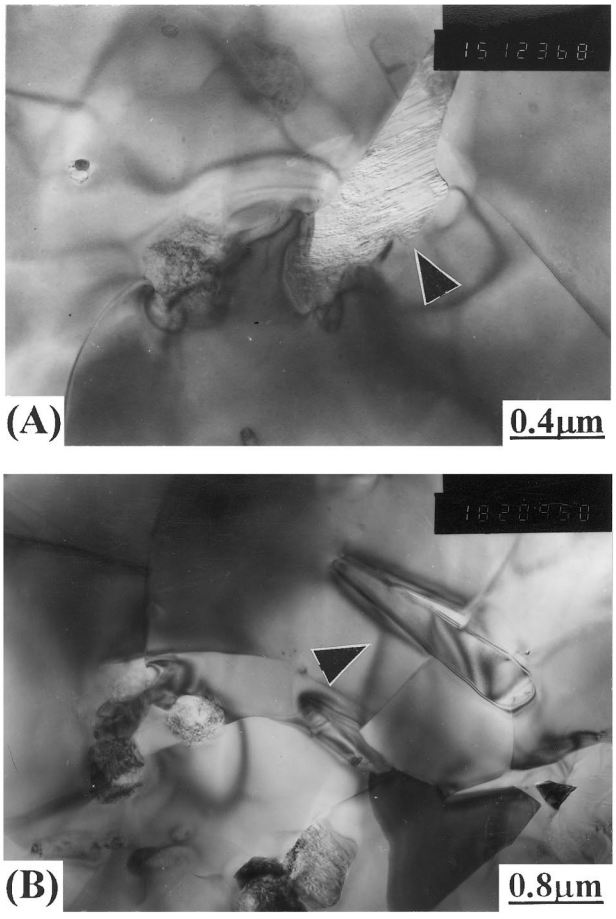

Fig. 4. TEM micrographs of (A) ASL1 and (B) ASL2, showing the pinning effect of irregular and elongated shaped SiC particles on Al_2O_3 grain boundaries (indicated by arrows).

one of the causes that the improvement in fracture mechanical properties of the composites at elevated temperature is more apparent than that at room temperature.

From the fracture morphology of the composites at room temperature, the fraction of transgranular fracture on the fracture surfaces are roughly estimated to be about $\alpha \approx 0{\cdot}5$ for the composites with 10 vol% SiC particles and $\alpha \approx 0{\cdot}9$ for the composites with 20 vol% SiC particles. At the same time, the transgranular fracture fraction for the composites at elevated temperature is assumed to be the same as that at room temperature, and set $\Delta K_R = 0$ at $T = 1200°C$. The predicted fracture toughness for the composites at room and elevated temperature is also listed in Tables 1 and 2, respectively, which indicate that the predicted toughness is qualitatively in agreement with the experimental data. In Table 1, the predicted toughness at room temperature exceeds the measured value, which may results from the fact that the one-dimensional stress toughening model of eqn (2) underestimates the effect of residual stress on the fracture toughness.[6] If a three-dimensional fluctuating stress field (as exists in the real materials) is considered, the residual stress in the composites should reduce the toughness larger, and the predicted toughness in Table 1 should decrease. In Table 2, it can be also found that the predicted toughness at elevated temperature is smaller than the measured value. The difference between the measured and predicted toughness at elevated temperature may be attributed to the bridging of SiC and Al_2O_3 grains, especially for ASL1. Because the thermal residual stress in the composites at elevated temperature is removed, and the grain boundaries soften and the bonding of grain boundaries weakens, which make the SiC and Al_2O_3 grains with elongated shapes pull-out possible. Since most of the Al_2O_3 grains in ASL1 are elongated, and the improvement in fracture toughness of ASL1 at elevated temperature is most apparent.

3.4 Creep behavior of composites

Figure 5 shows stress dependencies of steady-state or minimum creep rates for monolithic Al_2O_3 and the composites with 20 vol% SiC particles at $T = 1200°C$. Apparent linear fitting indicates that the stress exponent of monolithic Al_2O_3 is 1·45, and the stress exponents of ASS2 and ASL2 are 6·38 and 4·18, respectively. The stress exponents of ASS2 and ASL2 approach those of SiC whisker reinforced Al_2O_3 matrix composites[17,18] and are larger than that of Al_2O_3–SiC nanocomposites,[5] similar to the situation of ASS1 and ASL1.[12] From Fig. 5, it can be seen that the strain rate of ASS2 and ASL2 is lower than that of monolithic Al_2O_3 in the low stress region, especially for ASL2 with the strain rate 4∼8 times lower than that of monolithic Al_2O_3. If the effect of grain size on the strain rate ($\dot{\varepsilon} \propto 1/d^p$) is considered,[19] the strain rate of ASS2 and ASL2 should be lowered further, because the matrix grain sizes of ASS2 and ASL2 are smaller than that of monolithic Al_2O_3. As no

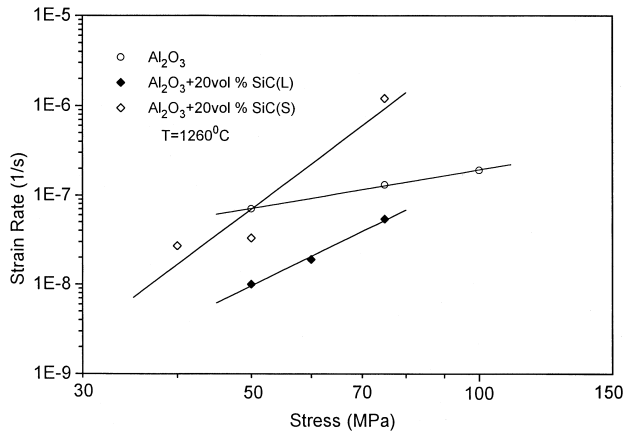

Fig. 5. Stress dependencies of steady-state or minimum creep rate for monolithic Al_2O_3 and the composites at $T = 1200°C$. The stress exponent for strain rate is 1·45 for monolithic Al_2O_3, 6·38 and 4·18 for ASS2 and ASL2, respectively.

dislocation motion was found in the crept specimens of monolithic Al_2O_3 and composites,[12,20] the boundary creep mechanisms are predominant[19] and the grain size exponent (p) should vary from 1 to 3. Recently, Lin *et al.*[21] studied the matrix grain size effect on creep behavior of 10 vol% SiC whisker reinforced Al_2O_3 matrix composites and found that the grain size exponent is approximate to 1. In fact, the matrix grain shape has no apparent change during creep tests in our observations,[12,20] and the grain size exponent of 1∼2 is reasonable[19] for our Al_2O_3 ceramic materials. Table 1 shows the ratios of matrix grain size of monolithic Al_2O_3 to that of the composites with $p = 1$. Considered the matrix grain size effect, the difference in strain rate between ASS2 and ASL2 should be reduced, but in general, the strain rate of ASL2 is also lower than that of ASS2 yet.

Grain boundary sliding facilitated by boundary diffusion is the predominant creep deformation mechanism of polycrystalline Al_2O_3 at temperature below 1400°C.[22,23] In our TEM observations,[12,20] it was found that there are some cavities at triple grain junctions or grain boundaries on the tensile sides of crept monolithic Al_2O_3 and composite specimens, and the shape of Al_2O_3 matrix grain experienced no apparent change during creep tests. Therefore, grain–boundary sliding, accommodated mainly by diffusion and still some unaccommodated, is the principal creep mechanism in the present Al_2O_3 ceramic materials.

The creep results of previous investigation[12] indicated that the creep resistance of ASL1 is much superior to that of monolithic Al_2O_3, due to its elongated grain morphology and good high temperature oxidation resistance. However, the composites with 20 vol% SiC particles also exhibited some improvement in their creep resistance, especially for ASL2, compared with the creep behavior of monolithic Al_2O_3, though their grain morphology is equiaxed and the SiC particles are not entrapped into Al_2O_3 matrix grains. The boundary SiC particles are easily to be oxidized[4,12] and form the viscous amorphous film on grain boundaries or triple grain junctions at elevated temperature during creeping, which is helpful to facilitate grain–boundary sliding and decrease the interface bonding, and decrease the creep resistance of the composites. The severe oxidation behavior of the composites can be seen from the cross sections of crept composite specimens, as shown in Fig. 6, where there is an apparent surface oxidation layer on the crept ASS2 and ASL2 specimens. The improvement mechanisms in creep resistance of ASS2 and ASL2 may be due to the pinning effect of irregular and elongated shaped SiC particles on Al_2O_3 grain boundaries, because these SiC particles

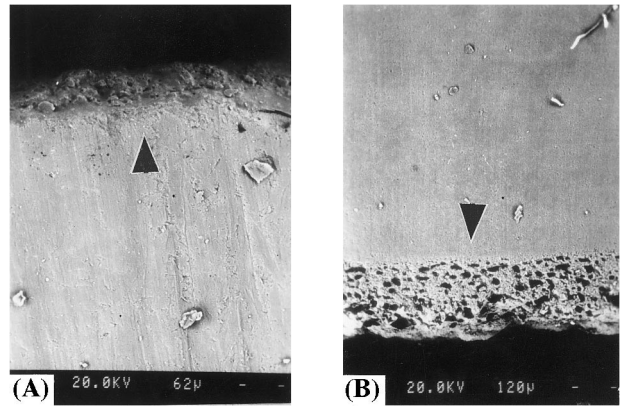

Fig. 6. SEM micrographs of the cross-sections of crept composite specimens prepared by mechanical fracture and grinding: (A) ASS2 specimen crept for 45 h at T = 1200°C and 50 MPa; (B) ASL2 specimen crept for 114 h at T = 1260°C≤ and 50 MPa, showing an apparent oxidation layer induced by carbon monoxide bubbles (indicated by arrows).

would inhibit the grain-boundary sliding during creeping and reduce the creep strain rate of the composites, similar to the reinforcing effect of whiskers.[17,18,22] At the same time, the pinning of 2·7 μm SiC particles on Al_2O_3 grain boundaries may be more effective than that of 0·6 μm SiC particles, due to the larger particle size, and the improvement in creep resistance of ASL2 is more apparent than that of ASS2. It is expected that the creep resistance of the composites should be enhanced further in inert atmosphere.

4 Conclusions

We have investigated the fracture mechanical properties of monolithic Al_2O_3 and Al_2O_3–SiC composites at room and elevated temperature, and the creep behavior of monolithic Al_2O_3 and the composites with 20 vol% SiC particles at T = 1260°C. The following results are obtained:

1. The fracture strength and toughness of the composites increase with the increase in the content of SiC particles, and the improvement in strength and toughness of the composites at elevated temperature is more apparent than that at room temperature, especially for ASL1 (with 10 vol% 2·7 μm SiC particles) with high temperature fracture toughness exceeding that of monolithic Al_2O_3 by over 90%.
2. The enhancement in fracture mechanical properties of the composites is due to the fracture mode change from intergranular in monolithic Al_2O_3 to transgranular in the composites, which is believed to result from the pinning effects of the irregular and elongated SiC particles on Al_2O_3 grain boundaries.

3. The superior high-temperature fracture mechanical properties of the composites are caused by the pullout mechanisms of elongated Al_2O_3 and SiC grains, due to the removal of thermal residual stress and the weakening of grain boundaries at elevated temperature. Because most of the Al_2O_3 grains in ASL1 are elongated, and its fracture toughness at elevated temperature is the best among the composites.
4. The composites with 20 vol% SiC particles exhibited some improvement in their creep resistance, especially for ASL2 (with 20 vol% 2·7 μm SiC particles), compared with the creep behavior of monolithic Al_2O_3, which is also believed to be due to the pinning SiC particles inhibiting Al_2O_3 grain–boundary sliding during creeping.

References

1. Niihara, K., New design concept of structural ceramics–ceramic nanocomposites. *Journal of the Ceramic Society Japan*, 1991, **99**(10), 974–982.
2. Stearns, L. C., Zhao, J. H. and Harmer, M. P., Processing and microstructure development in Al_2O_3–SiC nanocomposites. *Journal of the European Ceramic Society*, 1992, **10**, 473–477.
3. Zhao, J. H., Stearns, L. C., Harmer, M. P., Chan, H. M., Miller, G. A. and Cook, R. E., Mechanical behavior of alumina–silicon carbide nanocomposites. *Journal of the American Ceramic Society*, 1993, **76**(2), 503–510.
4. Piciacchio, A., Lee, S. H. and Messing, G. L., Processing and microstructure development in alumina–silicon carbide intragranular particulate composites. *Journal of the American Ceramic Society*, 1994, **77**(8), 2157–2164.
5. Ohji, T., Nakahira, A., Hirano, T. and Niihara, K., Tensile creep behavior of alumina/silicon carbide nanocomposite. *Journal of the American Ceramic Society*, 1994, **77**(12), 3259–3262.
6. Levin, I., Kaplan, W. D., Brandon, D. G. and Layyous, A. A., Effect of SiC submicrometer particle size and content on fracture toughness of alumina–SiC nanocomposites. *Journal of the American Ceramic Society*, 1995, **78**(1), 254–256.
7. Thompson, A. M., Chan, H. M., Harmer, M. P. and Cook, R. E., Crack healing and stress relaxation in Al_2O_3–SiC nanocomposites. *Journal of the American Ceramic Society*, 1995, **78**(3), 567–571.
8. Fang, J. X., Chan, H. M. and Harmer, M. P., Residual stress relaxation in Al_2O_3–SiC nanocomposite. *Mater. Sci. Eng.*, 1995, **A195**, 163–167.
9. Ohji, T., Hirano, T., Nakahira, A. and Niihara, K., Particle/matrix interface and its role in creep inhibition in alumina/silicon carbide nanocomposites. *Journal of the American Ceramic Society*, 1996, **79**(1), 33–45.
10. Chou, I. A., Chan, H. M. and Harmer, M. P., Machining-induced surface residual stress behavior in Al_2O_3–SiC nanocomposites. *Journal of the American Ceramic Society*, 1996, **79**(9), 2403–2409.
11. Anya, C. C. and Roberts, S. G., Indentation fracture toughness and surface flaw analysis of sintered alumina/SiC nanocomposites. *Journal of the European Ceramic Society*, 1996, **16**, 1107–1114.
12. Deng, Z. Y., Zhang, Y. F., Shi, J. L. and Guo, J. K., Microstructure and flexure creep behaviour of SiC-particle reinforced Al_2O_3 matrix composites. *Journal of European Ceramic Society*, 1996, **16**, 1337–1343.
13. O'Donnell, H. L., Readey, M. J. and Kovar, D., Effect of glass additions on the indentation-strength behavior of alumina. *Journal of American Ceramic Society*, 1995, **78**, 849–856.
14. Deng, Z. Y., Shi, J. L., Zhang, Y. F., Lai, T. R. and Guo, J. K., Creep and creep-recovery behavior in silicon carbide particle reinforced alumina. *Journal of European Ceramic Society* (in press).
15. Hansson, T., Warren, R. and Wasen, J., Fracture toughness anisotropy and toughening mechanisms of a hot-pressed alumina reinforced with silicon carbide whiskers. *Journal of American Ceramic Society*, 1993, **76**(4), 841–848.
16. Taya, M., Hayashi, S., Kobayashi, A. S. and Yoon, H. S., Toughening of a particulate-reinforced ceramic–matrix composite by thermal residual stress. *Journal of American Ceramic Society*, 1990, **73**(5), 1382–1391.
17. Nutt, S. R., Lipetzky, P. and Becher, P. F., Creep deformation of alumina–SiC composites. *Mater. Sci. Eng.*, 1990, **A126**, 165–172.
18. Tuffe, S., Dubois, J., Jorand, Y., Fantozzi, G. and Barbier, G., Processing and fracture behaviour of hot pressed silicon carbide whisker reinforced alumina. *Ceram. Int.*, 1994, **20**, 425–432.
19. Cannon, W. R. and Langdon, T. G., Review creep of ceramics: Part 1, mechanical characteristics. *J. Mater. Sci.*, 1983, **18**, 1–50.
20. Deng, Z. Y., Ph.D. thesis, Shanghai Institute of Ceramics, 1996.
21. Lin, H. T., Alexander, K. B. and Becher, P. F., Grain size effect on creep deformation of alumina–silicon carbide composites. *Journal of American Ceramic Society*, 1996, **79**(6), 1530–1536.
22. Lipetzky, P., Nutt, S. R., Koester, D. A. and Davis, R. F., Atmospheric effects on compressive creep of SiC-whisker-reinforced alumina. *Journal of American Ceramic Society*, 1991, **74**(6), 1240–1247.
23. Lin, H. T. and Breder, K., Creep deformation in an alumina–silicon carbide composite produced via a directed metal oxidation process. *Journal of American Ceramic Society*, 1996, **79**(8), 2218–2220.